Study of Resonances in 1x25kV AC Traction Systems with External Balancing Equipment

Nadhir Mesbahi, Lluís Monjo, and Luis Sainz

***Abstract*- AC traction systems are 1x25 or 2x25 kV/50 Hz single-phase, non-linear, time-varying loads that can cause power quality problems such as unbalanced or distorted voltages. To reduce unbalance, external balancing equipment is usually connected to these systems, forming the Steinmetz circuit. Parallel resonances can occur in this type of circuits, exciting the harmonic emissions (below 2 kHz) of railway adjustable speed drives. This paper studies these resonances at pantograph terminals and provides analytical expressions to determine their harmonic frequencies. The expressions are validated from several traction systems in the literature and PSCAD simulations.**

***Index Terms*— Harmonic analysis, resonance, traction systems, Steinmetz circuit.**

I. Introduction

At present, there are different traction system power supplies and the most common are the 1x25 kV and 2x25 kV 50 Hz railway power systems [1] – [3]. Although 2x25 kV traction systems are spreading in high-speed railways because of their ability to meet high power requirements at higher voltages [3], [4], 1x25 kV traction systems are still operating in traditional and high-speed railways, [5] – [8]. These systems are single-phase, non-linear, time-varying loads closely connected to the utility power supply system, so they can damage power quality [9] – [14]. Special consideration must be given to unbalanced or distorted line consumed currents because of single-phase high power consumption of trains [13], [14] and harmonic emissions of their adjustable speed drives [4], [9] – [12].

Several methods have been developed to reduce unbalance in traction systems, such as the use of active external balancing equipment [13] – [15]. This method consists of connecting thyristor controlled reactances in delta configuration to the traction system. This set is commonly known as Steinmetz circuit, whose design aims to obtain reactance values to symmetrize traction system consumed currents [14, 15]. The recent development of power electronics allows the rapid variation of Steinmetz circuit reactances in order to compensate for the usual single-phase load fluctuations [15].

This research work has been supported by grant ENE2013-46205-C5-3-R.

Nadhir Mesbahi is with the Department of Electrical Engineering ,University of El-Oued, P.O. Box 789, El-Oued 39000, Algeria (e-mail: mesbahi12006@yahoo.fr). Ll. Monjo and L. Sainz are with the Department of Electrical Engineering, ETSEIB-UPC, Av. Diagonal 647, 08028 Barcelona, Spain (e-mails: lluis.monjo@upc.edu, sainz@ee.upc.edu).

Pulse width-modulated (PWM) drives are most widely used in modern locomotives to obtain unity power factor and reduced harmonic current content. Nevertheless, the harmonic problem remains important because of the 1 to 2 kHz frequency range of their injected currents, which is close to the converter switching frequency [5], [9], [11], [12]. This worsens in trains equipped with phase-controlled thyristor converters because they consume currents with low displacement power factor and rich frequency content below 450 Hz [7], [12]. The harmonic problem is even greater in the presence of resonance in the overhead feeders of the traction circuit as it can increase harmonic voltage distortion. Many works have studied experimentally and numerically the resonance problem at traction system pantograph terminals [6], [7], [11], [16] – [19]. However, few consider external balancing equipment and represent the traction system by its equivalent impedance at the fundamental frequency obtained from its power demand [15].

The present paper uses the framework in [15], [20] to investigate 1x25 kV railway power system resonances observed from the traction load at pantograph terminals considering external balancing equipment. Analytical expressions for characterizing resonance frequencies are provided and the influence of traction system parameters and train position on these resonances is analyzed. The proposed expressions are validated from PSCAD simulations of three traction systems in the literature where resonance frequencies are numerically and experimentally located.

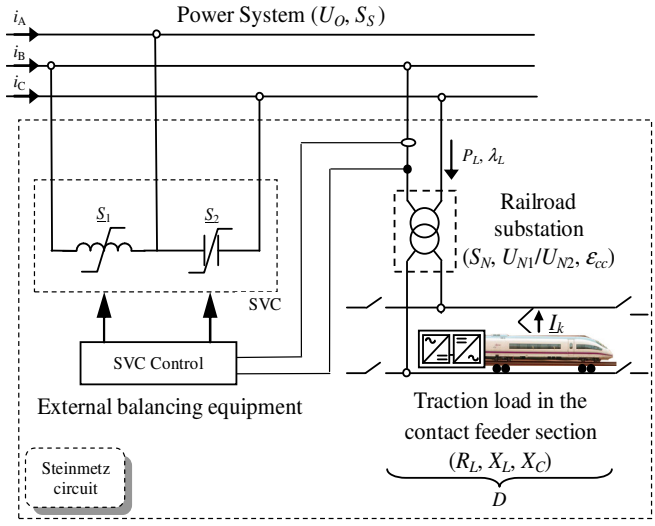

Fig. 1. Substation connection scheme of the 1x25kV AC traction system.

II. 1X25 KV SUPPLY OF AC TRACTION SYSTEMS

Many electrified traction systems operate at 1x25kV 50 Hz. In these systems, traction loads are supplied by single-phase overhead contact feeders distributed in different sections along the line. The usual length (D) of these sections is 30 or 40 km [8], [16], [17], [19] and they are connected to the main power network through the railroad substation transformer, Fig. 1. Active external balancing equipment could also be used to reduce current unbalance considering the usual fluctuations of traction loads. This equipment is based on static Var compensators (SVCs) and consists of thyristor controlled reactors (usually an inductor and a capacitor) delta-connected to the traction system. This set is known as Steinmetz circuit. In steady-state studies, railway traction systems are modeled with their equivalent circuit (Fig. 2), which is formed by,

- The power system: It is characterized from its open-circuit voltage U_O and short-circuit power S_S at the point of coupling. Since this short-circuit power is usually high, the short-circuit impedance is nearly zero, and so it could be neglected [2].
- The railroad substation U_{N1}/U_{N2} transformer: It is modeled from its rated power S_N and per-unit short-circuit impedance ε_{cc}.
- The contact feeder section of length D: Multiconductor transmission line theory and physical conductor models based on Carson's theory should be considered to accurately characterize the contact feeder section from the geometry and material properties of its wired connection structure [3], [4]. Nevertheless, it is too complicated to perform an analysis of railway electric system behavior based on formulas and equations with the above procedure. For this reason, the contact feeder section is represented with its "π" equivalent circuit dependent on traction load position with two cells at the left and right sides of the traction load. Each cell considers the per-unit-length longitudinal impedance of the line (i.e., R_L and X_L) and the per-unit-length parallel impedance between the line and the ground (i.e., X_C), whose values are usually obtained in the literature from multiconductor transmission line model simulations, experimental measurements in railway systems or Standards. These cells can be modeled in three ways [22]: (*i*) considering a distributed parameter model; (ii) considering a concentrated parameter model and using an n series "π" equivalent circuit; (*iii*) using a single "π" equivalent circuit with a concentrated parameter model, [16], [17]. The first model is used in the present Section to accurately characterize the harmonic response of the traction system. The third model is used in Section IV to analytically determine the resonance frequencies of the harmonic response. The goodness of the above approximation is checked in Section IV from the results obtained with the distributed parameter model.
- The external balancing equipment: The reactors of the equipment are usually an inductor whose associated resistance is commonly neglected and a capacitor, which are characterized by their power consumption $\underline{S}_1 \approx jQ_1$ $\underline{S}_2 = -jQ_2$, respectively. This consumption is determined from the traction system power consumption, which is characterized by the active power consumption P_L and the displacement power factor λ_L [15].

TABLE I
1X25KV 50 HZ TRACTION SYSTEM PARAMETERS [5], [6], [16] , [17], [19]

Power System	Open-circuit voltage	U_o	220, 132 kV
	Shot-circuit power	S_s	> 700MVA
Traction system	Active power consumption	P_L	$\approx N\cdot(8 \ldots 10)$ MW
	Displacement power factor	λ_L	$\approx 0.98 \ldots 1.0$
	Trains in section	N	3 … 6
Substation transformer	Transformer ratio	U_{N1}/U_{N2}	220 - 132/25 kV
	Rated power	S_N	12, 30, 60 MVA
	Short-circuit Impedance	ε_{cc}	$\approx 5 \ldots 12$ %
Contact feeder section	Longitudinal PI resistance	R_L	0.0125 ... 1.3125 Ω/km
	Longitudinal PI reactance	X_L	0.0625 ... 2.1875 Ω/km
	Transversal PI reactance	X_C	$1.2497\cdot10^5$ ... $1.5642\cdot10^6$ Ω·km
	Track length	D	30, 40 km

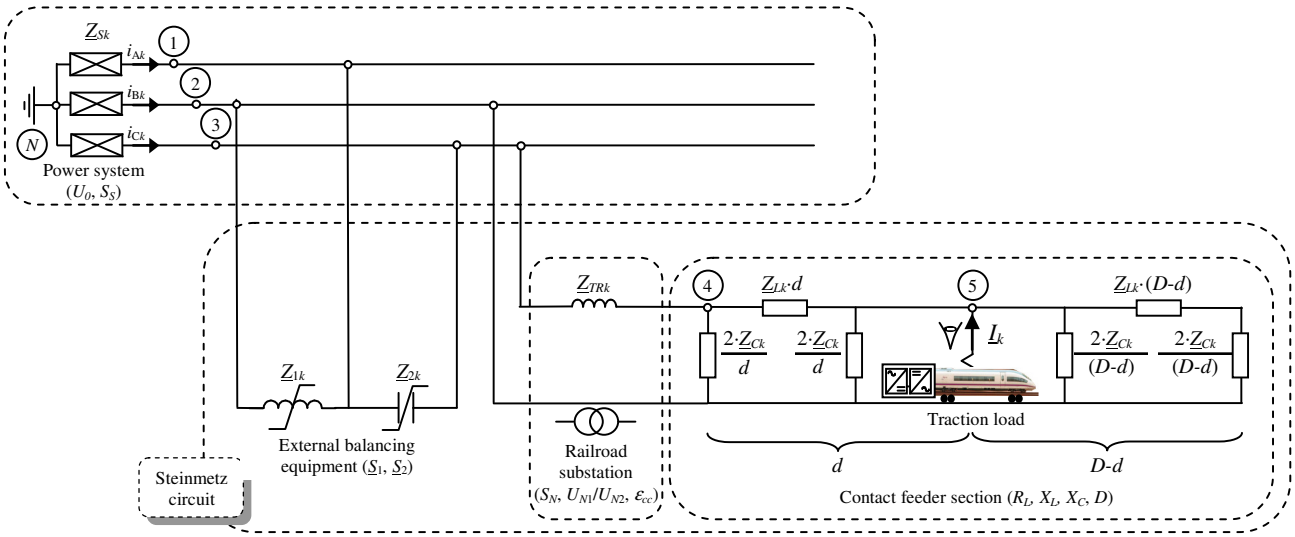

Fig. 2. Harmonic equivalent impedance circuit of the 1x25kV AC traction system.

The usual values of the above parameters are in Table I.

In railway traction systems, electric traction locomotives fed by adjustable speed drives are a source of harmonic currents $\underline{I}_k$ [7], [9], [13], [16], [17], which distort traction system voltages and reduces power quality. This can be increased by the presence of resonances in the system equivalent impedances [5], [8], [9]. To avoid this problem, the frequency of these resonances "observed" from the traction load at pantograph terminals must be determined. This is analyzed in the next Sections.

III. Traction System Harmonic Analysis

The harmonic behavior of the passive set "observed" from the traction load is studied in Fig. 2 to determine its harmonic response and resonance frequencies. This set is formed by the impedances (or admittances) of the power system, the external balancing equipment, the railroad substation transformer and the contact feeder section:

- Power system admittance: It includes the admittance of the power supply and the short-circuit impedance of the three-phase transformer which feeds the traction system:

$$\underline{Y}_{Sk} = \underline{Z}_{Sk}^{-1} \approx \frac{1}{jkX_S} = \left(jk \frac{U_O^2}{S_S} \left(\frac{U_{N2}}{U_{N1}} \right)^2 \right)^{-1} \approx \left(jk \frac{U_{N2}^2}{S_S} \right)^{-1} . \quad (1)$$

- External balancing equipment admittances: They are the inductor and capacitor admittances, which are obtained by considering traction system power consumption and forcing the current unbalance factor of the three-phase fundamental currents consumed by the Steinmetz circuit (i_{A1}, i_{B1}, i_{C1} in Fig. 2) to be zero [15]:

$$\underline{Y}_{1k} = \underline{Z}_{1k}^{-1} \approx \frac{1}{jkX_1} = \left(jk \frac{U_O^2}{Q_1} \left(\frac{U_{N2}}{U_{N1}} \right)^2 \right)^{-1} \approx \left(jk \frac{\sqrt{3} \cdot U_{N2}^2}{P_L \Lambda_{+1}} \right)^{-1}$$
$$\underline{Y}_{2k} = \underline{Z}_{2k}^{-1} = \frac{jk}{X_2} = jk \left(\frac{U_O^2}{Q_2} \left(\frac{U_{N2}}{U_{N1}} \right)^2 \right)^{-1} \approx jk \left(\frac{\sqrt{3} \cdot U_{N2}^2}{P_L \Lambda_{-1}} \right)^{-1} , \quad (2)$$

where

$$\Lambda_\xi = 1 + \xi \sqrt{3} \sqrt{\frac{1}{\lambda_L^2} - 1} \qquad (\xi = +1, -1). \quad (3)$$

- Railroad substation transformer admittance: It represents the short-circuit impedance of the transformer, which feeds the contact feeder section:

$$\underline{Y}_{TRk} = \underline{Z}_{TRk}^{-1} \approx \frac{1}{jkX_{TR}} = \left(jk \varepsilon_{cc} \frac{U_{N2}^2}{S_N} \right)^{-1} . \quad (4)$$

- Contact feeder section admittances: They represent the per-unit-length longitudinal and transversal impedances of the distributed parameter model [22]:

$$\underline{Y}_{Lk} = \underline{Z}_{Lk}^{-1} = \underline{Z}_{L\ell k}^{-1} \frac{\underline{\gamma}_{\ell k} \ell}{\sinh(\underline{\gamma}_{\ell k} \ell)}$$
$$\underline{Y}_{Ck} = \underline{Z}_{Ck}^{-1} = \underline{Y}_{C\ell k} \frac{\tanh(\underline{\gamma}_{\ell k} \ell/2)}{\underline{\gamma}_{\ell k} \ell/2} \qquad (\ell = d, D-d), \quad (5)$$

where

$$\underline{\gamma}_{\ell k} = \sqrt{\underline{Z}_{L\ell k} \cdot \underline{Y}_{C\ell k}} \qquad \underline{Z}_{L\ell k} = R_L + jkX_L \qquad \underline{Y}_{C\ell k} = j \frac{k}{X_C} . \quad (6)$$

The resistances of the power system and substation transformer impedances are neglected in the study because it is well-known that they damp the system harmonic response but do not modify the resonance frequencies significantly [15], [20].

Considering point N in Fig. 2 as the reference bus, the harmonic behavior of the system can be characterized by the admittance matrix [15], [20]:

$$\underline{\mathbf{V}}_\mathbf{k} = \underline{\mathbf{Z}}_{\mathbf{Busk}} \cdot \underline{\mathbf{I}}_\mathbf{k} \quad \Rightarrow \quad \begin{bmatrix} \underline{V}_{1k} \\ \vdots \\ \underline{V}_{5k} \end{bmatrix} = \begin{bmatrix} \underline{Z}_{11k} & \cdots & \underline{Z}_{15k} \\ \vdots & \ddots & \vdots \\ \underline{Z}_{51k} & \cdots & \underline{Z}_{55k} \end{bmatrix} \begin{bmatrix} 0 \\ \vdots \\ \underline{I}_k \end{bmatrix} =$$
$$\begin{bmatrix} \underline{Y}_{11k} & -\underline{Y}_{1k} & -\underline{Y}_{2k} & 0 & 0 \\ -\underline{Y}_{1k} & \underline{Y}_{22k} & 0 & -d\underline{Y}_{Ck}/2 & -\underline{Y}_{25k} \\ -\underline{Y}_{2k} & 0 & \underline{Y}_{33k} & -\underline{Y}_{TRk} & 0 \\ 0 & -d\underline{Y}_{Ck}/2 & -\underline{Y}_{TRk} & \underline{Y}_{44k} & -\underline{Y}_{Lk}/d \\ 0 & -\underline{Y}_{25k} & 0 & -\underline{Y}_{Lk}/d & \underline{Y}_{55k} \end{bmatrix}^{-1} \begin{bmatrix} 0 \\ 0 \\ 0 \\ 0 \\ \underline{I}_k \end{bmatrix} , \quad (7)$$

where

$$\underline{Y}_{11k} = \underline{Y}_{Sk} + \underline{Y}_{1k} + \underline{Y}_{2k}$$
$$\underline{Y}_{22k} = \underline{Y}_{Sk} + \underline{Y}_{1k} + d\underline{Y}_{Ck} + \frac{(D-d)\underline{Y}_{Ck}}{2} + \underline{Y}_{s2k}$$
$$\underline{Y}_{33k} = \underline{Y}_{Sk} + \underline{Y}_{2k} + \underline{Y}_{TRk} \qquad \underline{Y}_{44k} = \underline{Y}_{TRk} + \frac{d\underline{Y}_{Ck}}{2} + \frac{\underline{Y}_{Lk}}{d}$$
$$\underline{Y}_{55k} = \frac{d\underline{Y}_{Ck}}{2} + \frac{\underline{Y}_{Lk}}{d} + \frac{(D-d)\underline{Y}_{Ck}}{2} + \underline{Y}_{s2k} \quad (8)$$
$$\underline{Y}_{25k} = \frac{d\underline{Y}_{Ck}}{2} + \frac{(D-d)\underline{Y}_{Ck}}{2} + \underline{Y}_{s2k}$$
$$\underline{Y}_{s2k} = \frac{(\underline{Y}_{Lk}\underline{Y}_{Ck}/2)}{(\underline{Y}_{Lk}/(D-d) + (D-d)\underline{Y}_{Ck}/2)} ,$$

where d is the train position along the contact feeder section.

From (6) the equivalent harmonic impedance, which relates the k^{th} harmonic currents and voltages at the pantograph node (i.e., at node 5 in Fig. 2), can be obtained as follows:

$$\underline{V}_{55k} - \underline{V}_{22k} = (\underline{Z}_{55k} + \underline{Z}_{22k} - 2\underline{Z}_{25k})\underline{I}_k = \underline{Z}_{Eqk}\underline{I}_k . \quad (9)$$

The analysis of this impedance in a frequency range makes it possible to determine the resonance frequencies observed

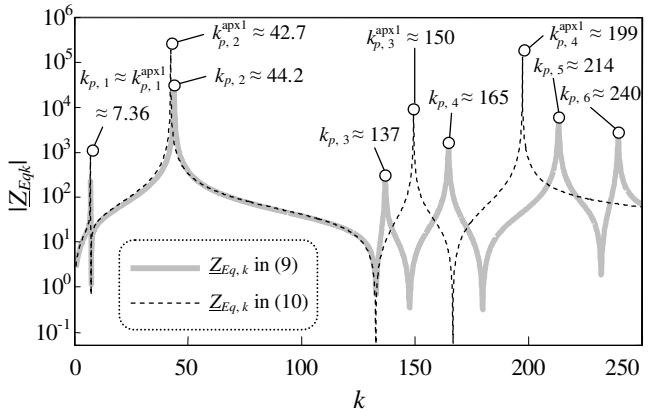

Fig. 3. Frequency response of the system equivalent impedance observed from the traction load when it is located at $d = D/2$ with $D = 30$ km.

TABLE II
1X25KV 50 HZ TRACTION SYSTEM RATIOS

Power System	Shot-circuit reactance	x_S (pu)	< 0.857
External balancing equipment	Inductor reactance	x_1 (pu)	≈ 43.3 … 17.3
	Capacitor reactance	x_2 (pu)	≈ 43.3 … 17.3
Contact feeder section	Longitudinal PI resistance	r_L (pu/km)	0.012 ... 1.26
	Longitudinal PI reactance	x_L (pu/km)	0.06 ... 2
	Transversal PI reactance	x_C (pu·km)	$1.2\cdot10^5$ ... $1.5\cdot10^6$

Note: The ratios are calculated from the following traction system values:
- Power system: U_O = 220 kV,
- Traction system: λ_L = 1.0,
- Substation transformer: S_N = 30 MVA, ε_{cc} = 5 % (i.e., X_{TR} = 1.04 Ω)

for the traction load. As an example, the solid gray line in Fig. 3 represents the frequency response of the equivalent impedance $\underline{Z}_{Eqk}$ numerically obtained from (7) and (9) considering the positions of the train at $d = D/2$ (with D = 30 km), its power consumption P_L = 24 MW and λ_L = 1.0 and the impedance values X_s = 0.417 Ω (S_S = 1500 MVA), X_{TR} = 1.04 Ω (S_N = 30 MVA and ε_{cc} = 5 %), R_L = 0.0232 Ω/km, X_L = 0.0625 Ω/km and $X_C = 1.25\cdot10^5$ Ω·km. Track length, power consumption and impedance values are obtained from the usual traction system parameters in Table I. The impedance $\underline{Z}_{Eqk}$ in Fig. 3 has the typical parallel resonances at pantograph terminals in the literature (i.e., $k_{p,2}$, $k_{p,3}$, $k_{p,4}$, $k_{p,5}$ and $k_{p,6}$) and a new parallel resonance (i.e., $k_{p,1}$) caused by the external balancing equipment. It must be highlighted that only the first and second resonances at $k_{p,1} \approx 7.36$ and $k_{p,2} \approx 44.2$ (i.e., $f_{p,1} \approx 368$ Hz and $f_{p,2} \approx 2.2$ kHz, respectively) can be truly problematic because of their proximity to the harmonic current emissions of the train converters [5], [9], [11], [12], [16], [17].

In the following Section, the impedance $\underline{Z}_{Eqk}$ is analytically determined and simple expressions to locate the above resonance frequencies are obtained.

IV. ANALYTICAL CHARACTERIZATION OF TRACTION SYSTEM HARMONIC RESPONSE

A. Traction System Harmonic Impedance

The impedance $\underline{Z}_{Eqk}$ is obtained from (7) and (9) after several mathematical operations. It is normalized with respect to the substation transformer reactance in order to reduce the number of variables in the study:

$$\underline{Z}_{Eqk,N} = \frac{\underline{Z}_{Eqk}}{X_{TR}} = \frac{1}{X_{TR}}\left(\frac{\underline{Y}_{Ck}(D-d)\left(4\underline{Y}_{Lk} + (D-d)^2\,\underline{Y}_{Ck}\right)}{2\left(2\underline{Y}_{Lk} + (D-d)^2\,\underline{Y}_{Ck}\right)} + \frac{2\underline{Y}_{Pk}\,\underline{Y}_{Lk} + d\cdot\underline{Y}_{Ck}(d\cdot\underline{Y}_{Pk} + \underline{Y}_{Lk})}{2(d\cdot\underline{Y}_{Pk} + \underline{Y}_{Lk})} \right)^{-1}, \tag{10}$$

where

$$\underline{Y}_{Pk} = \frac{\underline{Y}_{Fk}\,\underline{Y}_{TRk}}{\underline{Y}_{Fk} + \underline{Y}_{TRk}} + \frac{d}{2}\underline{Y}_{Ck}$$
$$\underline{Y}_{Fk} = \frac{(\underline{Y}_{Sk}/3 + \underline{Y}_{1k})(\underline{Y}_{Sk}/3 + \underline{Y}_{2k})}{(\underline{Y}_{Sk}/3 + \underline{Y}_{1k}) + (\underline{Y}_{Sk}/3 + \underline{Y}_{2k})} + \frac{\underline{Y}_{Sk}}{3}. \tag{11}$$

Expression (10) can also be obtained by simple inspection from the load terminals of the circuit in Fig. 2.

It is easy to demonstrate that the normalized impedance $\underline{Z}_{Eqk,N}$ only depends on the following terms:

$$X_{TR}\underline{Y}_{Sk} \approx \frac{X_{TR}}{jkX_S} = -j\frac{1}{kx_S}, \quad X_{TR}\underline{Y}_{TRk} \approx \frac{X_{TR}}{jkX_{TR}} = -j\frac{1}{k}$$
$$X_{TR}\underline{Y}_{1k} \approx \frac{X_{TR}}{jkX_1} = -j\frac{1}{kx_1}, \quad X_{TR}\underline{Y}_{2k} = j\frac{kX_{TR}}{X_2} = j\frac{1}{kx_2}$$
$$X_{TR}\underline{Y}_{Lk} = \frac{X_{TR}}{R_L + jkX_L} = \frac{1}{r_L + jkx_L}\frac{\underline{\gamma}_{xk}\cdot x}{\sinh(\underline{\gamma}_{xk}\cdot x)}$$
$$X_{TR}\underline{Y}_{Ck} = j\frac{kX_{TR}}{X_C}\frac{\tanh(\underline{\gamma}_{xk}\cdot x/2)}{\underline{\gamma}_{xk}\cdot x/2} = j\frac{k}{x_C}\frac{\tanh(\underline{\gamma}_{xk}\cdot x/2)}{\underline{\gamma}_{xk}\cdot x/2} \tag{12}$$
$$\underline{\gamma}_{xk} = \sqrt{\frac{\underline{Z}_{Lxk}}{X_{TR}}\cdot X_{TR}\underline{Y}_{Cxk}} = \sqrt{(r_L + jkx_L)\cdot j\frac{k}{x_C}}$$
$$x = d,\ D-d,$$

and therefore the magnitude of the normalized impedance $\underline{Z}_{Eqk,N}$ only depends on the harmonic order k , track length D, train position d and six ratios $x_S = X_S/X_{TR}$, $x_1 = X_1/X_{TR}$, $x_2 = X_2/X_{TR}$, $r_L = R_L/X_{TR}$, $x_L = X_L/X_{TR}$ and $x_C = X_C/X_{TR}$. Table II shows typical values of these ratios derived from the data in Table I. In the next Section, simple expressions to locate the resonance frequencies of $\underline{Z}_{Eqk}$ (or $\underline{Z}_{Eqk,N}$) based on ratios x_S, x_1, x_2, x_L and x_C are determined.

B. Analytical Determination of Resonance Frequencies

The resonance frequencies of $\underline{Z}_{Eqk,N}$ could be analytically determined by equating to zero the denominator in (10). However, the expression of this denominator is too complicated and the two approximations below must be made.

The distributed parameter model in (5) is approximated with the concentrated parameter model [22], i.e.:

$$\underline{Y}_{Lk} \approx \underline{Z}_{L\ell k}^{-1} = \frac{1}{R_L + jkX_L} \qquad \underline{Y}_{Ck} \approx \underline{Y}_{C\ell k} = j\frac{k}{X_C}. \tag{13}$$

It is well-known that the goodness of the above approximation depends on frequency range and cable length (i.e., contact feeder section length).

From (1) and (2) and according to the data of Table I, it can be observed that the reactance X_1 is much greater than the short-circuit reactance X_S:

$$\frac{X_1}{X_s} = \left(\frac{\sqrt{3}\cdot U_{N2}^2}{P_L\Lambda_{+1}}\right)\cdot\left(\frac{U_{N2}^2}{S_S}\right)^{-1} = \frac{\sqrt{3}\cdot S_S}{P_L\Lambda_{+1}} > 20.21, \tag{14}$$

and therefore, considering that X_1 and X_s are connected in parallel, $\underline{Y}_{Fk}$ in (10) can be approximated as

$$\underline{Y}_{Fk} \approx \frac{\underline{Y}_{Sk}/3(\underline{Y}_{Sk}/3 + \underline{Y}_{2k})}{\underline{Y}_{Sk}/3 + (\underline{Y}_{Sk}/3 + \underline{Y}_{2k})} + \frac{\underline{Y}_{Sk}}{3}. \tag{15}$$

To validate the analytical expression of $Z_{Eqk,N}^{\text{apx1}}$ (i.e., the expression of $\underline{Z}_{Eqk,N}$ in (10) considering (13) and (15)), Fig. 3 compares its frequency response (dashed black line) with that calculated in Section III. It can be observed that the resonances closest to the harmonic current emissions of the train converters (i.e., the first and second resonances $k_{p,1}$ and $k_{p,2}$) can be accurately characterized from the above approximation.

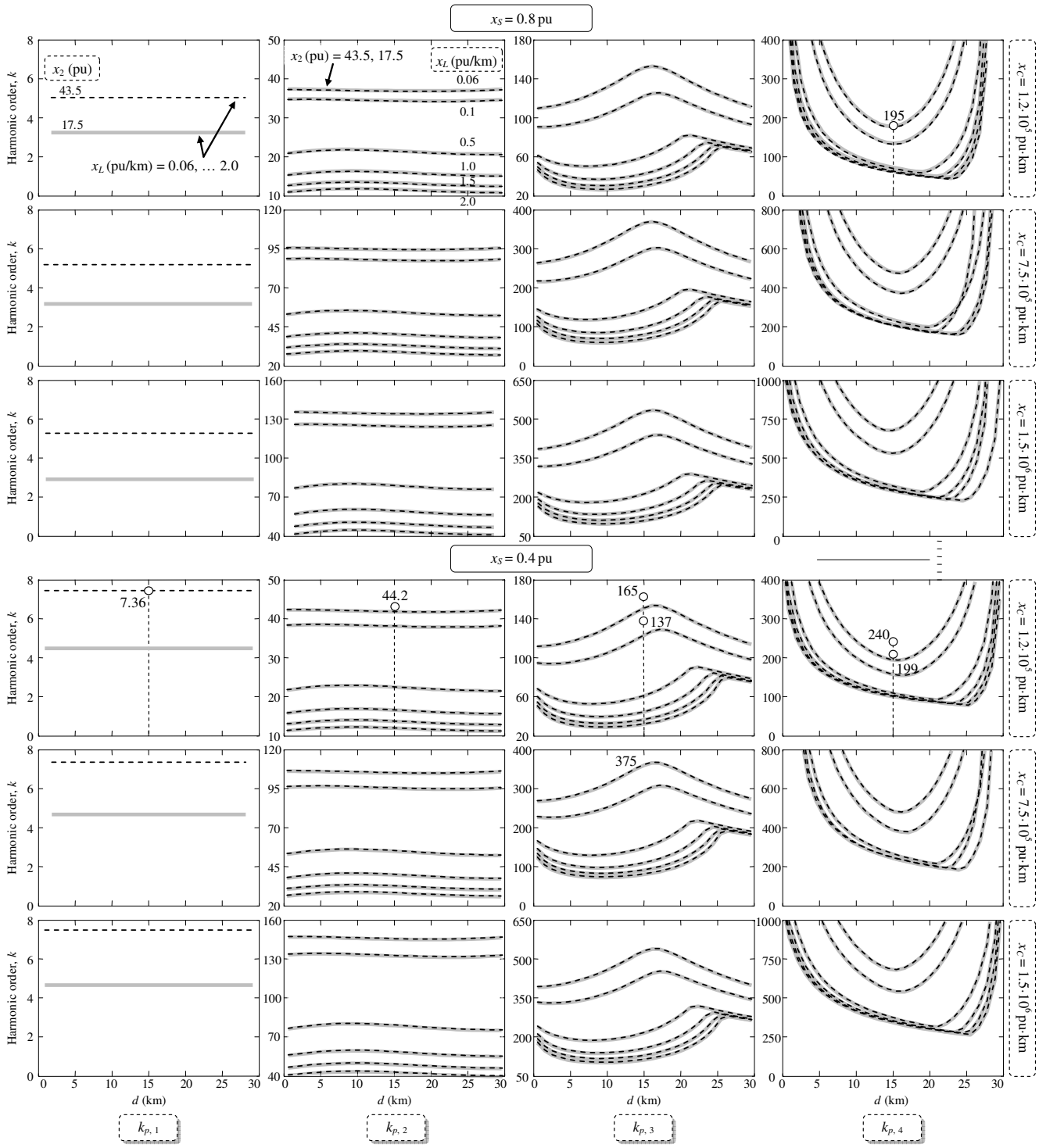

Fig. 4. Location of the resonance frequencies as a function of traction system ratios and train position along a contact feeder section of length D = 30 km.

On the other hand, this is not true for the other resonances (i.e., $k_{p,3}$, $k_{p,4}$, $k_{p,5}$ and $k_{p,6}$) due to the inaccuracy of the concentrated parameter model for these resonance frequencies. However, Fig. 3 shows that the resonance frequencies obtained with $Z_{Eqk,N}^{\text{apx1}}$ could provide a useful insight into high order resonance frequency range. These results can be approximately extended to any value of the system ratios in Table II.

The above approximation allows arranging the denominator of the approximated expression in the following form:

$$\text{Den}\left(\underline{Z}_{Eqk,N}^{\text{apx1}}\right) \approx c_4 k^8 + c_3 k^6 + c_2 k^4 + c_1 k^2 + c_0, \qquad (16)$$

where the coefficients of the equation are

$$
\begin{aligned}
c_4 &= x_L^2 x_S D d^2 \left(D-d\right)^2 \left(3x_S+2\right) \\
c_3 &= -D x_L \Big[x_2 x_L d^2 \left\{D-d\right\}^2 \\
&\quad + x_S \left\{ x_L \left(2d(D-d)^2(2x_C+x_2 d)\right) \right. \\
&\quad \left. + 2x_C (D^2 - Dd + d^2)(3x_S+2) \right\} \Big] \\
c_2 &= 2x_C D \Big[4x_C x_S \left\{3x_S + D x_L + 2\right\} \\
&\quad + x_L \left\{ x_2 \left(x_L d(D-d)^2 + (2x_S+1)(D^2 - Dd + d^2) \right) \right\} \Big] \\
c_1 &= -4x_C^2 \left[D x_2 \left\{ D x_L + 4x_S + 2 \right\} + 4 x_S x_C \right] \\
c_0 &= 8 x_2 x_C^3
\end{aligned}
\tag{17}
$$

In the above study, resistance R_L (i.e., ratio r_L) is neglected to reduce the number of the variables involved because it is proved that, as expected, this resistance damps the system harmonic response but does not affect the resonance frequency location significantly [15], [20]. The solutions of the polynomial function in (16) correspond to four real roots which allow determining the parallel resonance frequencies. These solutions can be obtained by the Descartes method [21] and are expressed as

$$
\begin{aligned}
k_{p,1-2}^{\text{apx1}} &= \sqrt{\frac{\sqrt{-m_1 \pm \sqrt{m_1^2 - 4m_3}}}{2} - \frac{c_3}{4c_4}} \\
k_{p,3-4}^{\text{apx1}} &= \sqrt{\frac{\sqrt{m_1 \pm \sqrt{m_1^2 - 4m_2}}}{2} - \frac{c_3}{4c_4}},
\end{aligned}
\tag{18}
$$

where

$$
\begin{aligned}
m_1 &= \sqrt{\frac{3(n_1^2 - 4n_3) - 4n_1^2}{3n_6} - \frac{2n_1}{3} - \frac{n_6}{3}} \\
m_2 &= \frac{n_1 + n_1^2 + n_2/n_1}{2} \qquad m_3 = m_2 - \frac{n_2}{m_1},
\end{aligned}
\tag{19}
$$

and

$$
\begin{aligned}
n_1 &= \frac{c_2}{c_4} - \frac{3(c_3/c_4)^2}{8} \qquad n_2 = \left(\frac{c_3}{2c_4}\right)^3 - \frac{c_3 c_2}{2c_4^2} + \frac{c_1}{c_4} \\
n_3 &= -3\left(\frac{c_3}{4c_4}\right)^4 + \frac{c_3^2 c_2}{16 c_4^3} - \frac{c_3 c_1}{4c_4^2} + \frac{c_0}{c_4} \\
n_4 &= 16 n_1^3 - 18 n_1 (n_1^2 - 4n_3) - 27 n_2^2 \\
n_5 &= \sqrt{n_4^2 - 4(4n_1^2 - 3(n_1^2 - 4n_3))^3} \qquad n_6 = \left(\frac{n_5 + n_4}{2}\right)^{1/3}.
\end{aligned}
\tag{20}
$$

Fig. 4 shows the harmonics of the parallel resonance frequencies in (18) as a function of train position d along the contact feeder section of length D = 30 km and the ratio range in Table II. They are calculated considering six values of ratio x_L (x_L = 0.06, 0.1, 0.5, 1.0, 1.5 and 2.0 pu/km), three values of ratio x_C ($x_C = 1.2\cdot10^5$, $7.5\cdot10^5$ and $1.5\cdot10^6$ pu·km), two values of ratio x_S (x_S = 0.4 and 0.8 pu) and two values of ratio x_2 (x_2 = 17.5 and 43.5 pu). Note that the gray and black lines correspond to the six values of x_L and x_2 = 17.3 and 43.3 pu, respectively. The first resonance does not depend on x_L, and therefore the lines of the six x_L values are overlapped. The other resonances do not significantly depend on x_2 and the gray and black lines of the six x_L values are practically overlapped. The resonances in the example of Section III (x_s = 0.4 pu, r_L = 0.022 pu/km, x_L = 0.06 pu/km, $x_C = 1.2\cdot10^5$ pu·km, $x_1 = x_2$ = 43.3 pu and $d = D/2$ = 15 km) are also shown in Fig. 4 to verify the usefulness of (18) in resonance frequency determination despite using the concentrated parameter model of the contact feeder section and neglecting the contact feeder section line resistance R_L and the external balancing equipment inductance X_1. As can be seen in Fig. 4, the low order harmonic resonances (i.e., $k_{p,1}$ and $k_{p,2}$), which do not depend on train position, could be close to the harmonic emissions of the train converters (i.e., below the 40th harmonic order) for most values of ratios x_L and x_C and can be accurately predicted with $k_{p,i}^{\text{apx1}}$ (i = 1–2) in (18). By contrast, the other resonances (i.e., $k_{p,3}$, $k_{p,4}$, $k_{p,5}$ and $k_{p,6}$) are far from these emissions and their frequency range could be obtained from $k_{p,i}^{\text{apx1}}$ (i = 3–4) in (18). Thus, Fig. 4 shows that, according to the $k_{p,i}^{\text{apx1}}$ (i = 3) plot, $k_{p,3}$ could occur below the 40th harmonic order for x_L greater than 0.5 pu/km and the smallest values of x_C. It can also be observed that the resonance at $k_{p,1}$ mainly depends on the power system and external balancing equipment ratios (x_S and x_2) while the resonance at $k_{p,2}$ mainly depends on the contact feeder section ratios (x_L and x_C).

C. Study of the first and second parallel resonances

Although the parallel resonances in (18), which are illustrated in Fig. 3 and Fig. 4, are reported in the literature, only the first and second (i.e., $k_{p,1}$ and $k_{p,2}$) must be studied because of their proximity to the harmonic emissions of train converters. Accordingly, this Section analyzes the dependence of these resonances on traction system parameters and proposes two approximated expressions to locate them.

Based on the slight dependence of the first resonance on contact feeder parameters (R_L, X_L and X_C) and train position d (Fig. 4), its frequency can be approximately determined by simple inspection of the passive set formed by the power system and the external balancing equipment (see Fig. 2):

$$
\begin{aligned}
\underline{Z}_{Eq1k,N}^{\text{apx2}} &\approx \frac{1}{X_{TR}} \left(\frac{\underline{Y}_{Sk}/3\,(\underline{Y}_{Sk}/3 + \underline{Y}_{2k})}{\underline{Y}_{Sk}/3 + (\underline{Y}_{Sk}/3 + \underline{Y}_{2k})} + \frac{\underline{Y}_{Sk}}{3} \right)^{-1} \\
&= jk3x_S \left(\frac{k^2 3x_S - 2x_2}{k^2 6x_S - 3x_2} \right).
\end{aligned}
\tag{21}
$$

and the first resonance of $\underline{Z}_{Eqk,N}$ in (10) can be approximately located by equating to zero the denominator in (21):

$$
k_{p,1}^{\text{apx2}} = \sqrt{\frac{x_2}{2x_S}} = \sqrt{\frac{P_L \Lambda_{-1}}{2\sqrt{3} S_S}}.
\tag{22}
$$

Based on the slight dependence of the second resonance on the power system, external balancing equipment and train position d [2], [5], [10] (Fig. 4), its frequency can be roughly determined by neglecting the power supply and external balancing equipment reactances and placing the train at the beginning of the contact feeder section (i.e., d = 0 km) in the circuit of Fig. 2. As can be seen in the resulting circuit, the expression of the normalized equivalent impedance at the load terminals is

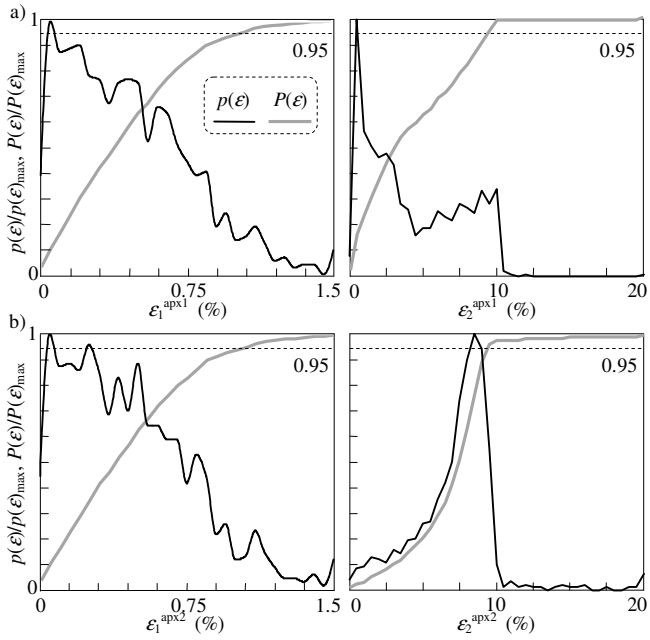

Fig. 5.Probability distribution and density functions of the errors of the approximated resonance frequency expressions.

$$\underline{Z}_{Eq2k,N}^{\text{apx 2}} = \frac{1}{X_{TR}}\, j\left(\frac{1}{kX_{TR}} - \frac{D\cdot k}{2X_C} + \frac{1}{\left(kX_L D - \dfrac{2X_C}{D\cdot k}\right)}\right)^{-1}, \quad (23)$$

where the longitudinal resistance of the contact feeder section line is not considered, in accordance with the previous Section. Thus, the second resonance of $Z_{Eqk,N}$ (10) can be approximately located by equating to zero the denominator in (23), which can be compacted as follows:

$$\text{Den}\left(\underline{Z}_{Eq2k,N}^{\text{apx 2}}\right) = x_L D^3\cdot k^4 - 2x_C D\cdot\left(D\cdot x_L + 2\right)\cdot k^2 + 4x_C^2, \quad (24)$$

and the second parallel resonance in (10) can be approximated by the following roots of equation (24):

$$k_{p,2}^{\text{apx 2}} = \frac{1}{D}\sqrt{\frac{x_C}{x_L}\left(D\cdot x_L + 2 - \sqrt{D^2\cdot x_L^2 + 4}\right)}. \quad (25)$$

D. Accuracy study of approximated expressions

The accuracy of the approximated expressions of the resonance frequencies $k_{p,i}^{\text{apx1}}$ and $k_{p,i}^{\text{apx2}}$ ($i = 1, 2$) in (18), (22) and (25) is discussed from 10000-shot Monte Carlo Matlab simulations. Uniform distributions of train position d along the contact feeder section of length $D = 30$ km and the traction system ratios according to the range in Table II are used in the simulations. To evaluate accuracy, the above resonance frequencies are determined from the 10000-shot random traction system values and the following errors are calculated:

$$\varepsilon_i^{\text{apxj}} = \frac{k_{p,i} - k_{p,i}^{\text{apx}\,j}}{k_{p,i}} \quad (j = 1,2 \quad ; \quad i = 1,2), \quad (26)$$

where $k_{p,i}$ is numerically obtained by equating to zero the denominator in (10), where the distributed parameter model of the contact feeder section is considered. The probability distribution and density functions $p(\varepsilon_i^{\text{apxj}})$ and $P(\varepsilon_i^{\text{apxj}})$ of the errors in (26) obtained from the Monte Carlo simulations are plotted in Fig. 5. It must be highlighted that the 95% percentile values of the $k_{p,1}^{\text{apxj}}$ and $k_{p,2}^{\text{apxj}}$ ($j = 1, 2$) errors are approximately below 1.5%, and 10%, respectively.

TABLE III
1X25KV 50 HZ TRACTION SYSTEMS IN THE LITERATURE

Ref.			[6]	[16]	[19]
Traction system	Train power consumption	P_L [MW]	1.5	2.5	1.6
	Displacement power factor	λ_L		… 1.0 …	
	Trains in section	N		… 2, 5 …	
Subst. transf.	Reactance	X_{TR} [Ω]	7.23	8.51	4.71
Contact feeder section	Long. π- resistance	R_L [Ω/km]	0.200	0.169	0.15
	Long. π-reactance	X_L [Ω/km]	0.4492	0.4335	0.3142
	Transv. π-reactance	X_C [Ω·km]	$1.55\cdot10^5$	$2.89\cdot10^5$	$2.12\cdot10^5$
	Track length	D	40	30	30
	Train position	d	20	10	30
Resonance	1^{st} ($k_{p,1}$)	[Ref]	---	---	---
		apx1	13.6, 8.9	10.0, 6.9	13.8, 9.0
		apx2	14.2, 9.0	11.0, 7.0	13.8, 8.7
	2^{nd} ($k_{p,2}$)	[Ref]	≈ 16	≈ 26	≈ 28
		apx1	16.9, 16,2	26.1, 26.1	27.8, 27.6
		apx2	16.7, 16,7	27.4, 27.4	29.6, 29.6
	3^{rd} ($k_{p,3}$)	[Ref]	≈ 49	≈ 90	≈ 70
		apx1	46.0, 47.0	74.4, 74.6	67.8, 67.7
	4^{rd} ($k_{p,4}$)	[Ref]	---	---	---
		apx1	69.8, 67.3	152.7, 151.7	600, 600

Note: "--- " means that no data are available.

E. Analysis of the parallel resonance results

According to the results obtained in the previous Sections, the following recommendations could be made to shift the first and second resonances from the harmonic current emissions of the train converter in 1x25 kV traction power systems:

- First parallel resonance $k_{p,1}$:
  - Traction power systems should be connected to main grids with high short-circuit powers. According to (23) and Fig. 4, higher short-circuit power levels of the main grid lead to higher frequencies of the first parallel resonance.
- Second parallel resonance $k_{p,2}$:
  - Contact feeder sections should have large per-unit-length parallel capacitances X_C and small per-unit-length longitudinal inductances X_L. According to (25) and Fig. 4, higher ratios $x_C = X_C/X_{TR}$ and smaller ratios $x_L = X_L/X_{TR}$ lead to higher frequencies of the second parallel resonance.
  - The length of contact feeder sections should be as short as possible (25). This cannot be concluded from Fig. 4 because it is plotted for a fixed length of the contact feeder section (i.e., $D = 30$ km).

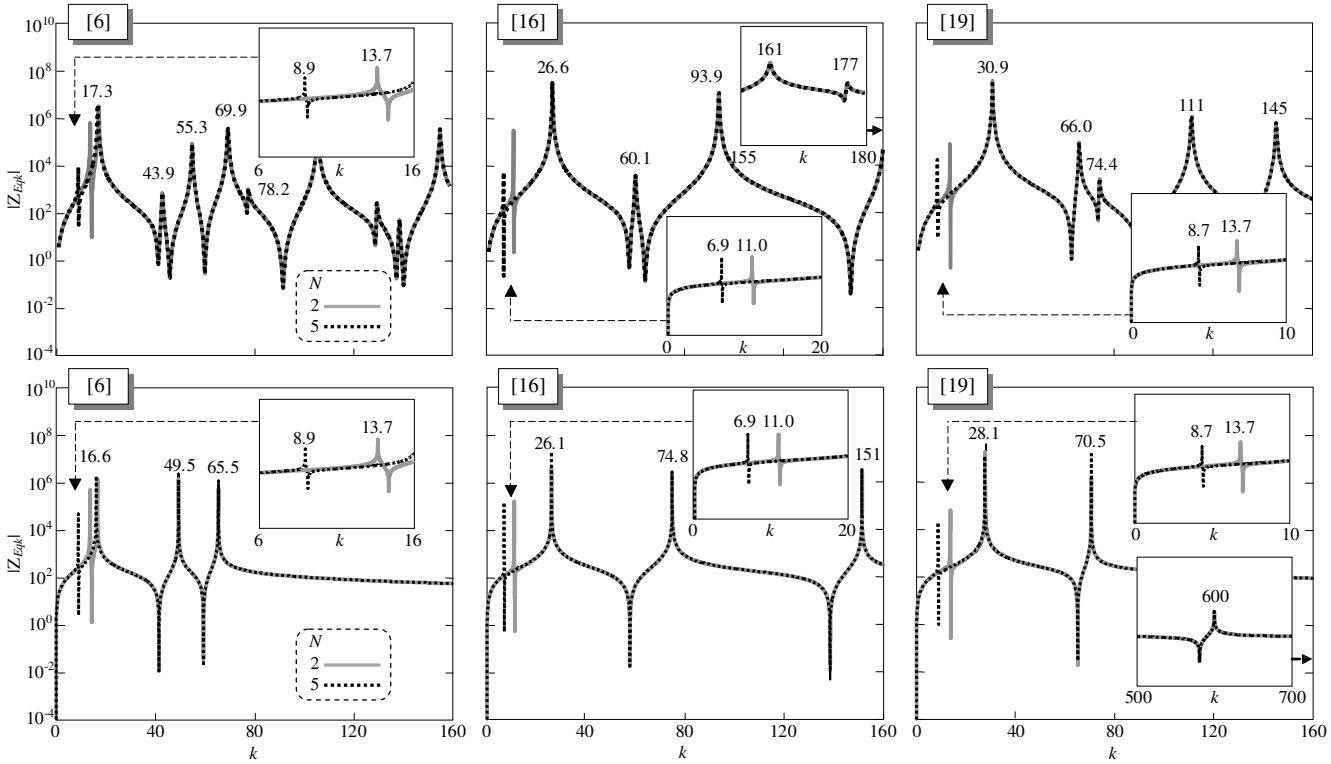

Fig. 6. Frequency response of the traction systems in the literature obtained from PSCAD simulations with distributed and concentrated parameter models of the ccontact feeder section (top and bottom, respectively).

- Main grids with high short-circuit powers can also help to shift parallel resonance (Fig. 4).

V. Application of Harmonic Resonance Location

The obtained expressions are applied to locate the harmonic resonance of three 1x25kV 50Hz traction power systems in the literature, [6], [16], [19].

In [6], harmonic study on the 40 km Velesin (Czech Republic) traction system is presented. The voltage and current waveforms reveal the presence of resonances in the traction system, which are analyzed from equivalent circuit simulations. In [16], a typical 1x25 kV 50 Hz traction substation with 30 km contact feeder sections is studied and electrical parameters are provided. In [19], technical details of a 30 km traction system such as harmonic distortion, resonance phenomena and AC filters are reported for different electrical system specifications.

Table III summarizes traction system electrical parameter data and the harmonic orders of parallel resonances provided by the above references. Although there is no information on the short-circuit power of the supply networks, a 700 MVA value is assumed. It is also assumed that external balancing equipment is connected to the power system and designed according to (2) to balance the power consumption of 2 or 5 trains. Considering these data, Fig. 6 shows the frequency response and resonance frequencies of the PSCAD simulations considering distributed and concentrated parameter models of the contact feeder sections (top and bottom, respectively). Furthermore, a harmonic study on parallel resonances is performed from the analytical expressions in Section IV and the results are reported in Table III, together with the results provided in the references. It must be noted that the first and second resonance results of the approximations agree with those in the original works and PSCAD simulations. With regard to the other resonance results, the approximation also agrees with those in the original works and PSCAD simulations with the concentrated parameter model. It also allows the frequency range of PSCAD results with the distributed parameter model to be obtained. However, this is not true in the study of reference [19], where $k_{p,4}^{\text{apx1}} = 600$ is far from $k_{p,5} = 111$ and $k_{p,6} = 145$ due to the long length of the contact feeder cell ($d = 30$ km) and the high frequency of $k_{p,4}^{\text{apx1}}$. The same example was analyzed with $d = 15$ km and the result of $k_{p,4}^{\text{apx1}}$ allowed the 5th and 6th resonance frequencies (i.e., $k_{p,5}$ and $k_{p,6}$) to be obtained. The study verifies that a larger number of trains (that is, higher traction system power consumption) leads to smaller external balancing equipment reactances (2), and therefore to lower first resonance frequencies (see Fig. 4). By contrast, the other resonances do not change significantly with the number of trains.

VI. Conclusions

The harmonic emissions of traction load converters can be magnified by the parallel resonances of the equivalent impedance observed from these converters. The paper gives analytical expressions to determine the harmonics at which these resonances occur in 1x25 kV 50 Hz traction systems with external balancing equipment. There are four parallel resonances but only the two lower ones, which are studied in detail, can be really dangerous because of their proximity to

the frequency of converter harmonic current emissions. These lower resonances do not depend on train position, which allows deriving a simpler expression to locate them. It is also observed that the first resonance mainly depends on the power system and balancing equipment while the second depends on the traction system. The proposed expressions are validated by analyzing the frequency response of several traction systems in the literature. The framework used to investigate the 1x25 kV railway power system resonances could be extended to other railway power systems (in particular, the 2x25 kV system, one of the most widespread). This framework mainly consists in modelling railway traction systems with their equivalent circuit, and subsequently obtaining the analytical expression of the equivalent harmonic impedance at the pantograph node. Commonly, the analysis of reasonable approximations in the equivalent circuit is also mandatory to simplify the study and obtain easy analytical expressions of the resonance frequencies.

VII. REFERENCES

[1] Steimel, A., "Electric Railway Traction in Europe," *IEEE Industry Applications Magazine,* November, 1996.

[2] E. Pilo, L. Rouco, A. Fernández, L. Abrahamsson, "A monovoltage equivalent model of bi-voltage autotransformer-based electrical systems in railways," *IEEE Trans. Power Del.*, vol. 27, no. 2, pp. 699-708, Jan. 2012.

[3] E. Pilo, R. Rouco, A. Fernández, A. Hernandez-Velilla, "A simulation tool for design of the electrical supply system of high-speed railway lines," *Proceedings of the IEEE Power Society Summer Meeting*,vol. 2, pp. 1053-1058, July. 2000.

[4] A. Dolara, M. Gualdoni, S. Leva, "Impact of high-voltage primary supply lines in the 2 x 25 kV – 50 Hz railway system on the equivalent impedance at pantograph terminals", *IEEE Trans. Power Del.*, vol. 27, no. 1, pp. 164-175, Jan. 2012.

[5] M.F.P. Janssen, P.G. Gonçalves, R.P. Santo, H.W.M. Smulders, "Simulations and measurements on electrical resonances on the Portuguese 25 kV network", WCRR Seoul, Korea, May 18-22, 2008

[6] V. Kolar et al., "Interference between electric traction supply network and distribution power network – Resonance phenomenon," *Proceedings of the 14th IEEE Int. Conf. on Harmonics and Quality of Power (ICHQP)*, pp. 1-4, Sept. 2010.

[7] S. K. N. Rajesh, O. Karunakara, K. Muthu, E. Nambudiri P.V.V., "Harmonic levels in a traction system - An overview," pp. 139–143.

[8] A. J. Griffin, "Methods of improving the voltage resgulation on 25kV electric railways," pp. 252–259, 1920.

[9] M. Brenna, A. Capasso, M. C. Falvo, F. Foiadelli, R. Lamedica, D. Zaninelli, "Investigation of resonance phenomena in high speed railway supply systems: Theoretical and experimental analysis", *Electric power systems research*, vol. 81, Issue 10, pp. 1915-1923, Oct. 2011.

[10] A. Capasso, R. Lamedica, S. Sangiovanni, G. Maranzano and A. Prudenzi, "Harmonics and PQ events monitoring in an electrified metro-transit system," *Int. Conf. on Harmonics and Quality of Power (ICHQP)*, vol. 2, pp. 441-446, Oct. 2002.

[11] P. Caramia, P. , Morrone, M., Verde, P., Varilone, "Interaction between Supply System and EMU Loco in 15kV-16 2/3 Hz AC Traction Systems," in *Proceedings of the Power Society Summer Meeting 2001*, vol. 1, pp. 198-203, 2001.

[12] O. Hamoud, "Harmonic problems in Queensland railway electric traction system," pp. 227–231, 1986.

[13] W. Qingzhu, W. Mingli, C. Jianye and Z. Guipping, "Optimal balancing of large single-phase traction load," *Proceedings of the IET Conference on Railway Traction Systems (RTS 2010)*, pp. 1-6, 2010.

[14] C. Arendse and G. Atkinson-Hope, "Design of a Steinmetz symmetrizer and application in unbalanced network," *Proceedings of the 45th International Universities Power Engineering Conference (UPEC)*, pp. 1-6, 2010.

[15] Ll. Monjo, L. Sainz and J. Rull, "Statistical study of resonance in AC traction systems equipped with Steinmetz circuit," Electric Power Systems Research, Vol. 103, pp. 223-232, Oct. 2013.

[16] P. Tan, P. C. Loh, and D. G. Holmes, "Optimal Impedance Termination of 25-kV Electrified Railway Systems for Improved Power Quality," vol. 20, no. 2, pp. 1703–1710, 2005.

[17] Guo, Q. Li, Y. Xu, "Study on harmonic resonance of traction line in electrified high-speed traction system" *Int.Conf. on Sustainable Power Generation and Supply (SUPERGEN)*, pp. 1-4, April 2009.

[18] A. Mariscorri, P. Pozzobon, M. Vanti, "Simplified modeling of 2x25-kV AT railway system for the solution of low frequency and large-scale problems", *IEEE Trans. Power Del.*, vol. 22, no. 1, pp. 296-301, Jan. 2007.

[19] L. Buhrkall, "Traction system case study," *Proceedings of the IET Professional Development course on Electric Traction Systems*, pp.45-63, Nov. 2008.

[20] L. Sainz, LL. Monjo, S. Riera and J. Pedra, **"**Study of Steinmetz circuit influence on AC traction system resonance," *IEEE Trans. on Power Delivery*, Vol. 27, Num. 4, pp. 2295-2303, 2012.

[21] J-P. Tignol, , "*Galois' theory of algebraic equations,*" MA, USA: World Scientific Publishing Co. Pte. Ltd., 2001.

[22] R. Langella, L. Nunges, F. Pilo, G. Pissano, G. Petretto, S. Scalari, A. Testa, "Preliminary analysis of MV cable line models for high frequency harmonic penetration studies", *Proceedings of the IEEE Power and Energy Society General Meeting*, pp. 1-8, 2011.